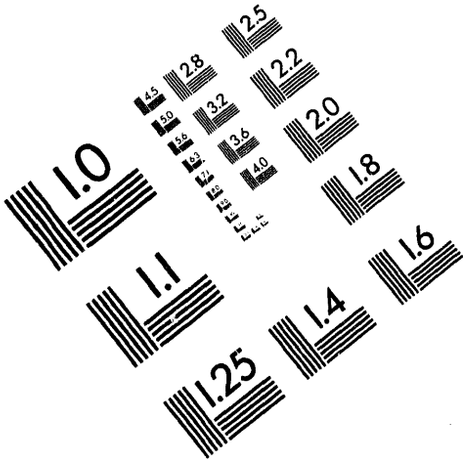

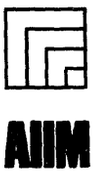

AIIM

**Association for Information and Image Management**

1100 Wayne Avenue, Suite 1100
Silver Spring, Maryland 20910

301/587-8202

Centimeter

1 2 3 4 5 6 7 8 9 10 11 12 13 14 15 mm

1 2 3 4 5

Inches

MANUFACTURED TO AIIM STANDARDS
BY APPLIED IMAGE, INC.

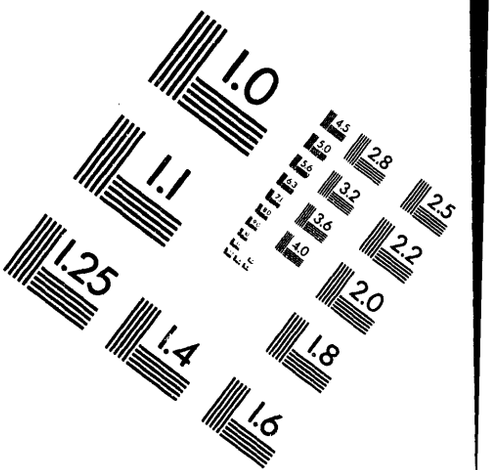

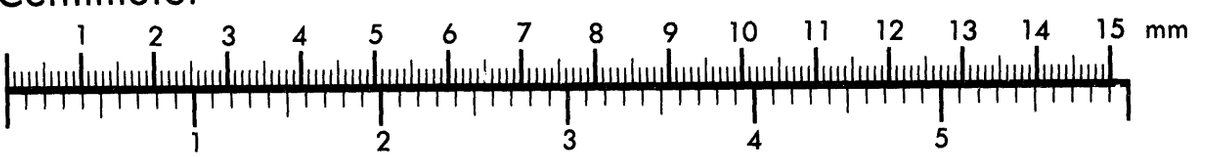

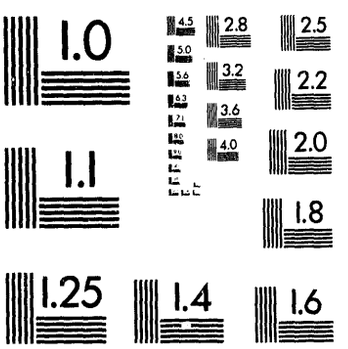

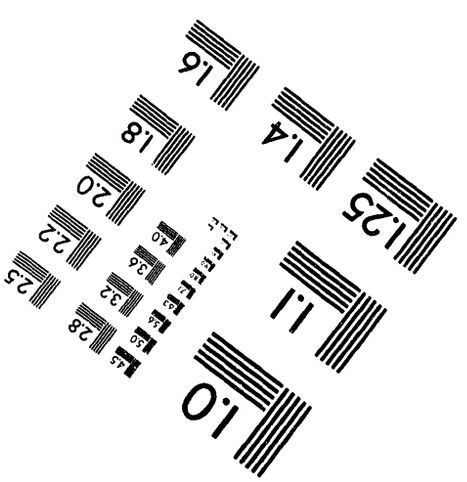

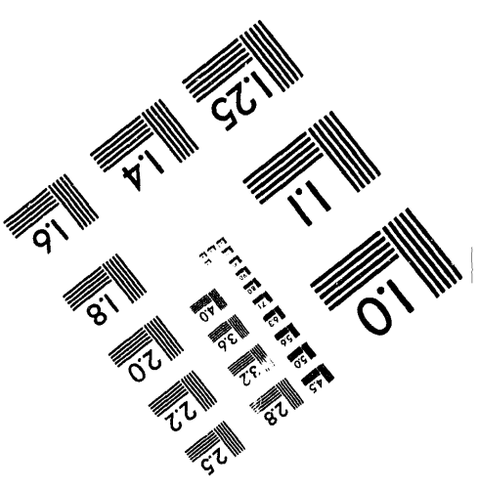

1 of 1

# Alpha particle effects on the internal kink mode

Yanlin Wu and C. Z. Cheng

Princeton Plasma Physics Laboratory, Princeton University

P.O. Box 451

Princeton, New Jersey 08540 USA

## Abstract

The $\alpha$-particle effects on the internal kink mode stability are studied. Finite Grad-Shafranov Shift, plasma $\beta$, and plasma shape can significantly enhance the trapped particle drift reversal domain in pitch angle space and reduce average magnetic drift frequency. The drift reversal effect on the ideal kink mode is small, but the $\beta_\alpha$ threshold for the fishbone mode can be much lower than previously predicted.[1] In addition, the ion diamagnetic drift has a stronger destabilizing effect.

MASTER



DISTRIBUTION OF THIS DOCUMENT IS UNLIMITED

The effects of energetic particles on the internal kink modes in tokamaks have been studied extensively.[1-5] Most of the previous works were focused on circular cross section systems and assumed a narrow hot particle pitch angle distribution. When the frequency $\omega$ is well below the energetic particle magnetic drift frequency $\omega_d$ and diamagnetic drift frequency $\omega_*$, the sign of the trapped hot particle potential energy is proportional to $\omega_*/\omega_d$, and the energetic trapped particles have a stabilizing effect if $\omega_*/\omega_d > 0$, and vice versa. As the hot particle beta $\beta_h$ is larger than a critical value, the fishbone mode appears with $\omega \sim \omega_d$. For fusion $\alpha$-particles, however, due to their uniform pitch angle distribution, $\omega_*/\omega_d$ may change from being positive to negative as the pitch angle changes from a deeply trapped state to a barely trapped state. The finite inverse aspect ratio $\varepsilon_a$, plasma $\beta$, and plasma shaping effects can enlarge the drift reversal domain. Thus, the net effect of trapped $\alpha$-particles must be integrated over entire trapped pitch angle domain. In this paper, we investigate $\alpha$-particle effects on the internal kink mode due to the magnetic drift reversal effect and the core ion finite Larmor radius effect through diamagnetic drift frequency. Although a particular Solovev equilibrium is used, we believe that the result from the study is qualitatively valid for general equilibria.

Consider an axisymmetric toroidal plasma, consisting of a core isotropic component and $\alpha$-particles with $n_\alpha \ll n_c$ and $T_\alpha \gg T_c$ but $\beta_\alpha \ll \beta_c$. The magnetic field for an axisymmetric toroidal system takes the form $\vec{B} = \nabla\phi \times \nabla\psi + I(\psi)\nabla\phi$, where $\psi$ is the poloidal flux and $\phi$ is the toroidal angle. We choose presure $p$ and $I(\psi)$ as $p = p_0 - p'\psi$ and $I^2 = I_0^2 + 2\delta R_0^2 p'\psi/(1+\kappa^2)$, where $p_0, p', R_0, \kappa$ and $I_0$ are positive constants, the prime refers to the $\psi$ derivative, and $\delta$ is a real constant. Here $\kappa$ describes the ellipticity, $\delta$ is the trangularity of the plasma shape, and $\kappa = 1$ and $\delta = 0$ represents a circular flux surface in the large aspect ratio limit. The exact solution of the Grad-Shafronov equation had been obtained by Solovev and is given by

$$\psi = [Z^2(R^2 - R_0^2\delta) + \frac{\kappa^2}{4}(R^2 - R_0^2)^2]\frac{p'}{2(1+\kappa^2)}. \tag{1}$$

Changing the coordinate system from $(R, Z, \phi)$ to $(\chi, \theta, \phi)$ by leting

$$\chi = \frac{1}{\kappa}\sqrt{Z^2(R^2 - R_0^2\delta) + \frac{\kappa^2}{4}(R^2 - R_0^2)^2}, \qquad \theta = \tan^{-1}(\frac{2}{\kappa}\frac{Z\sqrt{R^2 - R_0^2\delta}}{R^2 - R_0^2})$$

we have

$$\psi = \frac{\kappa^2 p'}{2(1+\kappa^2)}\chi^2, \qquad R = \sqrt{R_0^2 + 2\chi\cos\theta}, \qquad Z = \frac{\kappa\chi}{\sqrt{R^2 - R_0^2\delta}}\sin\theta.$$

The toroidal precessional drift frequency of a trapped particle can be expressed as[6] $\omega_d = \partial_\Psi J/\partial_E J$, where the longitudinal invariant $J = \oint v_\parallel d\ell$ involves an integral over the bounce orbit of a trapped particle, $v_\parallel = \sqrt{2(E - \mu B)}$ is the parallel velocity, $E = v^2/2$ is the energy, and $\mu$ is the magnetic moment. To the fist order in inverse aspect ratio the trapped particle toroidal precessional drift frequency is

$$\omega_d = (1+\kappa^2)\omega_{d0}\, g\, \chi_s/(\kappa^2\chi), \tag{2}$$

where $\omega_{d0} = 2E/(p' R_0^2 \chi_s)$, $\chi_s$ is the $\chi$ value at the $q = 1$ surface,

$$g = \frac{G_1 + \hat{s}G_2 - (\frac{4\kappa^2\delta}{(1+\kappa^2)^2}\bar{\beta}_p G_0 + 4G_3 - 5G_4)\varepsilon}{G_0 - 2\varepsilon G_1} \tag{3}$$

the average plasma poloidal beta is $\bar{\beta}_p = R_0^4 p'^2/(4B_0^2)$, $G_0 = K, G_1 = 2E - K, G_2 = 2E(k^2) - 2(1-k^2)K, G_3 = 2[(1-k^2)E(k^2) - (1-2k^2)K]/3, G_4 = [4(1-k^2)E + (4k^2-1)K]/3$, $K(k^2)$ and $E(k^2)$ are the complete elliptic integrals, $k^2 = (1 + \varepsilon - \lambda)/(2\varepsilon)$, $\lambda = \mu B_0/E$, $\hat{s} = (\chi/I)\partial_\chi I$, and $\varepsilon = \chi/R_0^2$ is the local inverse aspect ratio or the derivative of the Grad-Shafranov Shift ($\Delta' = \varepsilon$). For trapped particles we have $k^2 \leq 1$. The effect of ellipticity is mainly to reduce the magnitude of precessional drift frequency. Since $(3 - 4k^2 G_1)$ is positive for all pitch angle value, the finite Grad-Shafranov Shift, shaping factors $\kappa$ and $\delta$, and plasma $\beta$ will reduce the precessional drift frequency and broaden the drift reversal domain in the pitch angle space. The destablizing effect of the finite Grad-Shafranov Shift can be understood as particles spend longer time in the bad curvature region. The above

result is very similar to that of Connor et al.[7] Note that in the previous calculation of $\alpha$-particle effect on internal kink mode,[1] the effects due to finite $\beta$, plasma shaping, and inverse aspect ratio corrections were not included, and $\omega_d = \omega_{d0} G_1 \chi_s / \chi$ was used.

Figure 1 plots trapped particle domain in $(\varepsilon, \lambda)$ space and the $\omega_d = 0$ curve (Solid curve). For a given radial location, $\omega_d$ changes from being positive to negative as pitch $\lambda$ decreases, which means that $\omega_*/\omega_d$ also varies from being postitive to negative. If the trapped particles are destabilizing to a certain MHD mode for $\omega_*/\omega_d > 0$ in certain pitch angle region, the trapped particles in the pitch angle region with $\omega_*/\omega_d < 0$ would be stabilizing. Thus, the net effect of trapped $\alpha$-particles must be integrated over the entire trapped $\alpha$-particle population. If the drift reversal domain is large enough so that the net contribution from the term $\omega_*/\omega_d$ is negative, then the ideal MHD stable kink mode can be destabilized by the $\alpha$-particles. Also shown in Fig. 1 is the $\omega_d = 0$ curve (Dashed line) without the finite inverse aspect ratio $\varepsilon$, shaping factors $\kappa$ and $\delta$, and plasma $\beta$ effects. It is clear that the drift reversal domain increases due to these corrections.

Assuming a slowing-down distribution function with uniform pitch angle, the dispersion relation for the $n = 1$ internal kink mode is given by[1,2,8]

$$D(\omega) = -i\sqrt{\omega(\omega - \omega_{*i})} + \gamma_b + \tilde{\omega}_A \delta \hat{W}_k = 0 \tag{4}$$

where $\omega_{*i}$ is the ion diamagnetic drift frequency, $\tilde{\omega}_A$ is the shear Alfven frequency, and $\gamma_b$ is the ideal kink mode growth rate. Including the shapping effect $\gamma_b$ takes the form[9,10] $\gamma_b = 3\pi\tilde{\omega}_A(1 - q_0)[\beta_p^2 - 0.09/(1-\delta)^2] r_s^2/R^2$, with $\beta_p = -(R^2/r_s^4)\int_0^{r_s} r^2 \beta' dr$.

The normalized kinetic potential energy $\delta\hat{W}_k$ is mainly contributed by the trapped $\alpha$-particles and is given by

$$\delta\hat{W}_k = \frac{3}{4r_s^2}\int_0^{r_s} r\beta_\alpha(r)\, dr \int_{1-r}^{1+r} d\lambda \frac{k_2^2}{k_b}\{\frac{\omega_*}{\omega_d} + \frac{\omega}{\omega_d}(\frac{\omega_*}{\omega_d} - 1)S(\frac{\omega_d}{\omega})\},$$

where $r = \chi/R$, $k_b = \sqrt{2/r}K(k^2)/\pi$, $k_2 = \langle\cos(q\theta)\rangle$ which is a bounce-averaged quantity, and $S(\omega_d/\omega) = \ln(1 - \omega_d/\omega) + 2\pi i$ if $\gamma < 0$ and $0 < \omega_r/\omega_d \leq 1$, otherewise, $S(\omega_d/\omega) =$

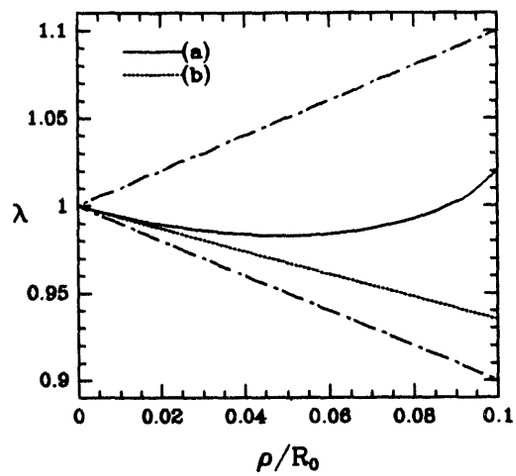


Figure 1: The $\omega_d = 0$ curves in the trapped particle $(r, \lambda)$ domain. Curve (a) uses the present $\omega_d = \omega_{d0} g$ with $\kappa = 1.5, \delta = 0.3$ and $\alpha = 0.5$, and curve (b) uses $\omega_d = \omega_{d0} \frac{\rho_s}{\rho} G_1$.

$\ln(1 - \omega_d/\omega)$.

The marginal stability condition can be understood by assuming a mean value $\bar{\omega}_d$ to approximate the pitch angle integral effect on $\omega_d$. The effect of magnetic drift reversal is to reduce the average precessional drift frequency $\bar{\omega}_d$. The marginal stability conditions for both the ideal kink and the fishbone modes are determined by $\omega(1 - \beta_\alpha^2 \sigma(\omega)^2/\beta_0^2) = \omega_{*i}$ and $\gamma_b = \beta_\alpha/(\pi\beta_0)(\bar{\omega}_d + \omega \ln \mid 1 - \bar{\omega}_d/\omega \mid)$, where $\beta_0 = 4\bar{\omega}_d^2/(3\pi\omega_*\tilde{\omega}_A)$. Since the number of trapped alpha particles satisfying resonance condition depends on $\omega, \sigma(\omega)$ represents the fraction of trapped alpha particles satisfying resonance condition and is less than one. Note that at $\beta_\alpha = 0$, the marginal stability for ideal kink is possible for $\omega_{*i}/2 \leq \omega_r \leq \omega_{*i}$ and $\gamma_b \leq \omega_{*i}/2$.

At marginal stability, the real frequency of the ideal kink mode is given by $\omega = \omega_{*i}/(1-$

$\beta_\alpha^2\sigma(\omega)^2/\beta_0^2$), and the stability boundary is given by

$$\gamma_b = \frac{3\omega_*\tilde{\omega}_A\beta_\alpha}{4\bar{\omega}_d}(1 + \frac{\omega_{*i}}{\bar{\omega}_d}\ln \mid 1 - \frac{\bar{\omega}_d}{\omega_{*i}} \mid). \tag{5}$$

As $\bar{\omega}_d$ decreases, the marginal stability boundary curve for the ideal kink mode has a steeper slope in the $(\beta_\alpha, \gamma_b)$ space. On the other hand, the contribution of $\omega_{*i}$ is to reduce $\gamma_b$ if $\mid 1 - \bar{\omega}_d/\omega_{*i} \mid < 1$, and vice versa.

At marginal stability the real frequency of the fishbone mode is much larger than $\omega_{*i}$, but smaller than $\bar{\omega}_d$, and is roughly given by $\omega = 0.78\bar{\omega}_d[1 - 0.3\gamma_b\bar{\omega}_d/(\beta_\alpha\omega_*\tilde{\omega}_A)]$ for $4\gamma_b\bar{\omega}_d/(3\beta_\alpha\omega_*\tilde{\omega}_A) \ll 1$. The marginal stability boundary is given by

$$\beta_\alpha\sigma(\omega) = \frac{4\bar{\omega}_d^2}{3\pi\omega_*\tilde{\omega}_A}\sqrt{1 - \frac{1.28\omega_{*i}}{\bar{\omega}_d}(1 + \frac{0.3\gamma_b\bar{\omega}_d}{\beta_\alpha\omega_*\tilde{\omega}_A})}. \tag{6}$$

Thus, for the fishbone branch, the effect of reducing $\bar{\omega}_d$ or increasing $\omega_{*i}$ is to reduce the critical $\beta_\alpha$, and vice versa.

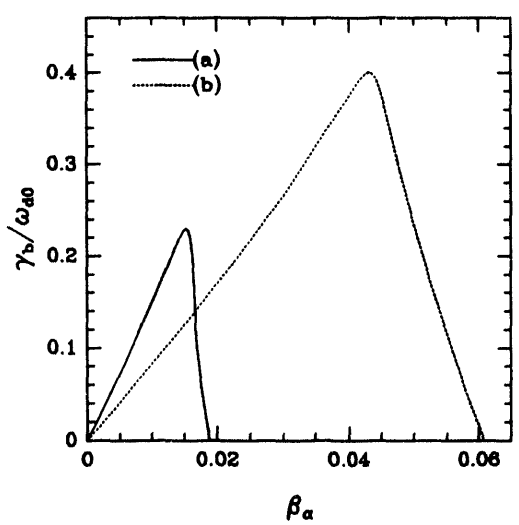


Figure 2: Marginal stability curves in the $(\beta_\alpha, \gamma_b)$ plane for $\omega_{*i} = 0$ and $\kappa = 1$. Curve (a) uses $\omega_d = \omega_{d0}g\ r_s/r$ with $\delta = 0.3$, and curve (b) uses $\omega_d = \omega_{d0}G_1\ r_s/r$.

In the following we present numerical solutions of the dispersion relation, Eq. (4). With the fixed parameters $E_\alpha = 3.5MeV$, $\omega_*/\omega_{d0} = \tilde{\omega}_A/\omega_{d0} = 10, r_s/R = 0.1, q_0 = 0.8$, Fig. 2 shows the marginal stability curves in $(\beta_\alpha, \gamma_b)$ space for $\omega_{*i} = 0$. In the domain under the curves, the plasma is stable; the left boundary is for the ideal kink mode, and the right boundary is for the fishbone mode. The solid curve is obtained by using $\omega_d = \omega_{d0} g\ r_s/r$, the dotted curve is obtained by using $\omega_d = \omega_{d0} G_1\ r_s/r$ (plasma beta and inverse aspect ratio effects are neglected), and the dashed line uses $\omega_d = \omega_{d0}\ r_s/r$ which represents the deeply trapped limit. Here $g < G_1 \leq 1$. It is clear that the drift reversal effect is reducing the average $\bar{\omega}_d$, and thus the critical $\beta_\alpha$ for both the ideal kink and the fishbone modes. The drift reversal has a small stabilizing effect on the ideal kink branch; the slope of the curve is proportional to $1/\bar{\omega}_d$ near $\beta_\alpha = 0$. However, the drift reversal has a large destabilizing effect on the fishbone mode; the threshold for the fishbone is substantially lowered since the critical $\beta_\alpha \sim \bar{\omega}_d^2$. We note that even when the total plasma $\beta$ is below the ideal internal kink threshold, the fishbone mode can be excited with large $\beta_\alpha$. The result for deeply trapped limit [(curve (c))] is presented for comparison purpose.

Figure 3 plots the marginal stability boundaries in the $(\beta_\alpha, \gamma_b)$ space for ellipticity $\kappa$ and trangularity $\delta$ dependences. The fixed parameters are the same as in Fig. 2. In general, as $\kappa$ or $\delta$ increases, the field line curvature and thus $\omega_d$ will decrease, which can be seen from Eq. (2). It is clear that as $\kappa$ or $\delta$ gets larger, the stable domain becomes narrower mainly due to the destabilizing effect on the fishbone mode. The $\beta_\alpha$ threshold for the stabilization of ideal kink mode is only slightly decreased by $\kappa$ and $\delta$. But, the threshold for the fishbone mode excitation can be significantly reduced by $\kappa$ and $\delta$. As pointed out by Kerner[9] and Connor,[10] the ideal magnetohydrodynamic (MHD) critical $\beta_{pc}$ and thus $\gamma_b$ depend weakly on the ellipticity $\kappa$, but strongly depend on the trianglarity $\delta$. For Solovev equilibrium[9] $\beta_{pc}$ is proportional to $(1-\delta)^{-1}$, and $\delta$ reduces $\gamma_b$. Since the marginal stability boundary for the ideal kink mode is only weakly modified by $\delta$, the effect of $\delta$ through $\gamma_b$

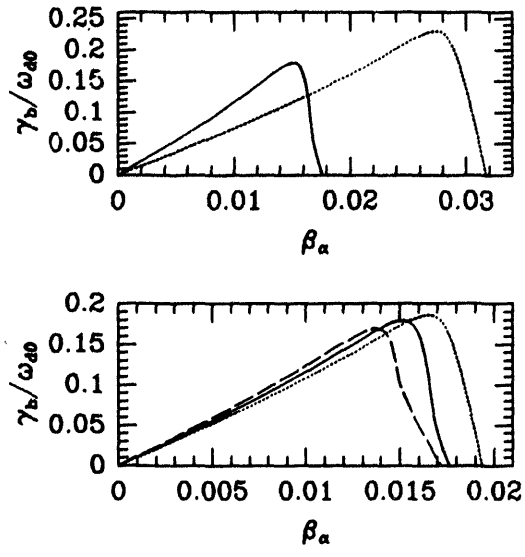


Figure 3: The ellipticity $\kappa$ and trangularity $\delta$ dependence of the marginal stability curves in the $(\beta_\alpha, \gamma_b)$ plane for $\omega_{*i} = 0$.

has a strong stabilizing effect on the ideal kink mode. On the other hand, the effect of $\delta$ through $\gamma_b$ competes with its destabilizing effect on the fishbone mode.

Figure 4 shows the core ion finite Larmor radius effect (finite $\omega_{*i}$) on the stability boundary in the $(\beta_\alpha, \gamma_b)$ space for $\kappa = 1.5$ and $\delta = 0.3$. For typical tokamak parameters we expect $\omega_{*i}/\omega_{d0} \leq 0.1$. As $\omega_{*i}$ increases the $\gamma_b$ threshold decreases for the ideal kink mode, but decreases much more for the fishbone mode. We note that the threshold for the ideal kink mode is reduced by $\omega_{*i}$. This is due to the increase of frequency and the decrease of $\omega_d$ so that there are more particles with $\omega_d \sim \omega_{*i}$ and $\mid 1 - \omega_d/\omega_{*i} \mid < 1$. Then, from our analytical theory [(Eq. (5))] the $\gamma_b$ threshold for the ideal kink mode is reduced by $\omega_{*i}$. For the fishbone mode the $\beta_\alpha$ threshold is further reduced by $\omega_{*i}$ as predicted from our analytical analysis. The results show that due to the magnetic drift reversal effect $\omega_{*i}$ reduces the stable domain much more than the previous calculation indicated.[1]

In summary, the effects of trapped fusion $\alpha$-particles on internal kink modes have

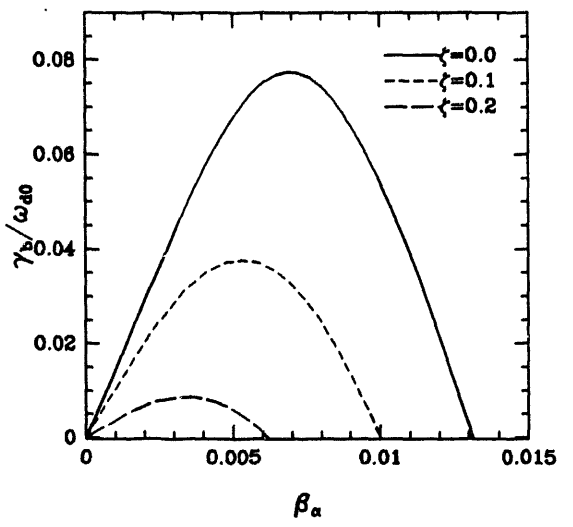


Figure 4: The diamagnetic drift frequency $\zeta(=\omega_{*i}/\omega_{d0})$-dependence of the marginal stability curves in the $(\beta_\alpha, \gamma_b)$ plane for $\kappa = 1.5$ and $\delta = 0.3$.

been investigated. Finite Grad-Shafranov Shift, plasma $\beta$, and plasma shaping effects can significantly enhance the trapped particle drift reversal domain in the pitch angle space and reduce the magnitude of the precessional drift frequency. The stable domain for both the ideal kink and the fishbone modes can be significantly reduced. For typical tokamak parameters, the core ion diamagnetic drift effect can narrow the stable domain in the presence of alpha particles, even though it has a stablizing effect in the ideal MHD limit.

One of the authors Yanlin Wu is grateful to Dr. R. B. White for useful discussions. This work was supported by the United States Department of Energy under contract number DE-AC02-76-CH03073.

## References


[1]B. Coppi, S. Migliuolo, F. Pegoraro, and F. Porcelli, Phys. Fluids B **2**, 927 (1990).

[2]L. Chen, R. B. White, and M. N. Rosenbluth, Phys. Rev. Lett. **52**, 1122 (1984).

[3]R. B. White, L. Chen, F. Romenelli, and R. Hay, Phys. Fluids B **28**, 278 (1985).

[4]C. Z. Cheng, Phys. Fluids B **2**, 1427 (1990).

[5]C. Z. Cheng, Phys. Reports **211**, 1 (1992).

[6]M. N. Rosenbluth and M. L. Sloan, Phys. Fluids **14**, 1726 (1971).

[7]J. W. Connor, R. J. Hastie, and T. J. Martin, Nucl. Fusion **23**, 1702 (1983).

[8]G. Ara, B. Basu, B. Coppi, G. Laval, M. N. Rosenbluth, and B. V. Waddell, Ann Phys. **112**, 443 (1975).

[9]W. Kerner, *Magnetohydrodynamic Instabilities for Tokamaks with Noncircular Cross Section*, PhD thesis, Plasma Physics Lab, Princeton University, 1975.

[10]J. W. Connor and R. J. Hastie, The effect of shaped plasma cross sections on the ideal internal kink mode in a tokamak, CLM-M106, 1985.

EXTERNAL DISTRIBUTION IN ADDITION TO UC-420

Dr. F. Paoloni, Univ. of Wollongong, AUSTRALIA
Prof. R.C. Cross, Univ. of Sydney, AUSTRALIA
Plasma Research Lab., Australian Nat. Univ., AUSTRALIA
Prof. I.R. Jones, Flinders Univ, AUSTRALIA
Prof. F. Cap, Inst. for Theoretical Physics, AUSTRIA
Prof. M. Heindler, Institut für Theoretische Physik, AUSTRIA
Prof. M. Goossens, Astronomisch Instituut, BELGIUM
Ecole Royale Militaire, Lab. de Phy. Plasmas, BELGIUM
Commission-European, DG. XII-Fusion Prog., BELGIUM
Prof. R. Bouciqué, Rijksuniversiteit Gent, BELGIUM
Dr. P.H. Sakanaka, Instituto Fisica, BRAZIL
Prof. Dr. I.C. Nascimento, Instituto Fisica, Sao Paulo, BRAZIL
Instituto Nacional De Pesquisas Espaciais-INPE, BRAZIL
Documents Office, Atomic Energy of Canada Ltd., CANADA
Ms. M. Morin, CCFM/Tokamak de Varennes, CANADA
Dr. M.P. Bachynski, MPB Technologies, Inc., CANADA
Dr. H.M. Skarsgard, Univ. of Saskatchewan, CANADA
Prof. J. Teichmann, Univ. of Montreal, CANADA
Prof. S.R. Sreenivasan, Univ. of Calgary, CANADA
Prof. T.W. Johnston, INRS-Energie, CANADA
Dr. R. Bolton, Centre canadien de fusion magnétique, CANADA
Dr. C.R. James,, Univ. of Alberta, CANADA
Dr. P. Lukác, Komenského Universzita, CZECHO-SLOVAKIA
The Librarian, Culham Laboratory, ENGLAND
Library, R61, Rutherford Appleton Laboratory, ENGLAND
Mrs. S.A. Hutchinson, JET Library, ENGLAND
Dr. S.C. Sharma, Univ. of South Pacific, FIJI ISLANDS
P. Mähönen, Univ. of Helsinki, FINLAND
Prof. M.N. Bussac, Ecole Polytechnique,, FRANCE
C. Mouttet, Lab. de Physique des Milieux Ionisés, FRANCE
J. Radet, CEN/CADARACHE - Bat 506, FRANCE
Prof. E. Economou, Univ. of Crete, GREECE
Ms. C. Rinni, Univ. of Ioannina, GREECE
Preprint Library, Hungarian Academy of Sci., HUNGARY
Dr. B. DasGupta, Saha Inst. of Nuclear Physics, INDIA
Dr. P. Kaw, Inst. for Plasma Research, INDIA
Dr. P. Rosenau, Israel Inst. of Technology, ISRAEL
Librarian, International Center for Theo Physics, ITALY
Miss C. De Palo, Associazione EURATOM-ENEA , ITALY
Dr. G. Grosso, Istituto di Fisica del Plasma, ITALY
Prof. G. Rostangni, Istituto Gas Ionizzati Del Cnr, ITALY
Dr. H. Yamato, Toshiba Res & Devel Center, JAPAN
Prof. I. Kawakami, Hiroshima Univ., JAPAN
Prof. K. Nishikawa, Hiroshima Univ., JAPAN
Librarian, Naka Fusion Research Establishment, JAERI, JAPAN
Director, Japan Atomic Energy Research Inst., JAPAN
Prof. S. Itoh, Kyushu Univ., JAPAN
Research Info. Ctr., National Instit. for Fusion Science, JAPAN
Prof. S. Tanaka, Kyoto Univ., JAPAN
Library, Kyoto Univ., JAPAN
Prof. N. Inoue, Univ. of Tokyo, JAPAN
Secretary, Plasma Section, Electrotechnical Lab., JAPAN
Dr. O. Mitarai, Kumamoto Inst. of Technology, JAPAN
Dr. G.S. Lee, Korea Basic Sci. Ctr., KOREA
J. Hyeon-Sook, Korea Atomic Energy Research Inst., KOREA
D.I. Choi, The Korea Adv. Inst. of Sci. & Tech., KOREA
Prof. B.S. Liley, Univ. of Waikato, NEW ZEALAND
Inst of Physics, Chinese Acad Sci PEOPLE'S REP. OF CHINA
Library, Inst. of Plasma Physics, PEOPLE'S REP. OF CHINA
Tsinghua Univ. Library, PEOPLE'S REPUBLIC OF CHINA
Z. Li, S.W. Inst Physics, PEOPLE'S REPUBLIC OF CHINA
Prof. J.A.C. Cabral, Instituto Superior Tecnico, PORTUGAL
Prof. M.A. Hellberg, Univ. of Natal, S. AFRICA
Prof. D.E. Kim, Pohang Inst. of Sci. & Tech., SO. KOREA
Prof. C.I.E.M.A.T, Fusion Division Library, SPAIN
Dr. L. Stenflo, Univ. of UMEA, SWEDEN
Library, Royal Inst. of Technology, SWEDEN
Prof. H. Wilhelmson, Chalmers Univ. of Tech., SWEDEN
Centre Phys. Des Plasmas, Ecole Polytech, SWITZERLAND
Bibliotheek, Inst. Voor Plasma-Fysica, THE NETHERLANDS
Asst. Prof. Dr. S. Cakir, Middle East Tech. Univ., TURKEY
Dr. V.A. Glukhikh,Sci. Res. Inst. Electrophys.I Apparatus, USSR
Dr. D.D. Ryutov, Siberian Branch of Academy of Sci., USSR
Dr. G.A. Eliseev, I.V. Kurchatov Inst., USSR
Librarian, The Ukr.SSR Academy of Sciences, USSR
Dr. L.M. Kovrizhnykh, Inst. of General Physics, USSR
Kernforschungsanlage GmbH, Zentralbibliothek, W. GERMANY
Bibliothek, Inst. Für Plasmaforschung, W. GERMANY
Prof. K. Schindler, Ruhr-Universität Bochum, W. GERMANY
Dr. F. Wagner, (ASDEX), Max-Planck-Institut, W. GERMANY
Librarian, Max-Planck-Institut, W. GERMANY

DATE
FILMED
9/26/94

END